

CHAPTER 6

Modeling Cellular Networks

Tae Jun Lee, Dennis Tu, Chee Meng Tan,
and Lingchong You

6.1 Introduction

Systems-level understanding of cellular dynamics is important for identifying biological principles and may serve as a critical foundation for developing therapeutic strategies. To date, numerous developments of therapeutics have been based on identification and comprehensive analysis of cellular dynamics, especially in the involved pathways. In cancer therapy, for instance, many researchers have focused on oncogenic pathways such as the Rb pathway, whose in-depth understanding of the pathway dynamics promises effective therapeutics [1–7]. The effectiveness of this approach in the development of cancer therapeutics has been illustrated in *in vivo* pre-clinical tests of the engineered adenovirus ONYX-015 and ONYX-411. These adenoviruses, engineered to target mutations in the Rb or p53 pathway for killing, have demonstrated high selectivity and efficiency in viral replication in tumor cells for cell killing [8, 9]. However, clinical application of these methods is hindered by lack of ability to precisely predict and regulate cellular responses. This ability is essential in minimizing complications and side effects. Especially, a large amount of biology data on these pathways generated by rapid advancements in biotechnologies and molecular biology renders integrated understanding of the pathway dynamics impossible by intuition alone. Therefore, a more systematic approach allowing incorporation of the multitude of information is necessary to improve prediction and regulation of cellular responses.

To this end, mathematical modeling is becoming increasingly indispensable for basic and applied biological research. Essentially, a mathematical model is a systematic representation of biological systems, whose analysis can confer quantitative predicting power. In recent years, advanced computing power combined with improved numerical methods have made it possible to simulate and analyze dynamics of complex cellular networks [10–19].

Mathematical modeling is useful in a number of ways. One of the common applications of mathematical modeling is to analyze cellular networks systematically. For example, although the mitogen-activated protein kinase (MAPK) was known to control multiple cellular responses such as cell growth, survival, or differentiation, the molecular mechanisms for these divergent behaviors were not fully elucidated.

Consequently, several models on the MAPK pathway have been developed that differentiate activation patterns in response to epidermal growth factors and neural growth factors [20], characterize the signal-response relationship [21, 22], and suggest the significance of feedback control in complete signal adaptation [23]. A more extensive modeling work investigates the emergent properties that arise from multiple signaling pathways [24]. These works illustrate the utility of mathematical modeling in understanding complex biological systems that intuition alone cannot handle.

Another use of mathematical modeling has been demonstrated in devising strategies to control cellular dynamics. The concentrations of MAPK phosphatase have been shown to play a key role in whether the MAPK pathway demonstrates monostable or bistable states [22]. Sasagawa and colleagues used their MAPK model to identify “critical nodes,” in which perturbations resulted in dramatic changes in system behaviors [20]. A number of critical nodes that are responsible for diverse cellular actions have also been suggested in the insulin-signaling pathways based on biochemical and computational data [25]. Such characterization of input-output response or identification of critical nodes can be utilized to effectively modulate cellular dynamics.

Furthermore, modeling can form a basis for the development of therapeutics for medical applications. Various pathway models including the MAPK models described above can be useful in designing, or evaluating the effectiveness of, therapeutic drugs *in silico* [20–24]. The predictive power and therapeutics design principles that these models offer can facilitate development of therapeutics [26–28]. Stemming from these studies on the MAPK signaling pathways, Kitano and colleagues have developed an EGFR pathway map in a software that is shared and compatible with other simulation and analysis packages [29]. Such efforts to make available and share information on biological pathways among researchers exemplify an inclination towards understanding of biology via mathematical modeling.

Despite advantages of mathematical modeling for basic and applied biological research, there remain many challenges in constructing and analyzing models. Modeling of biological systems is always accompanied by assumptions, which are predicated on the modeler’s goals. Therefore, a successful modeling work requires clear justification of these assumptions. Even with clear, justified goals, a modeler is faced with another challenge: lack of detailed, quantitative biological information. While biotechnologies continue to advance our knowledge of the building blocks of biological systems, parameters for the kinetics of interactions among them are often unknown. Various methodologies for inferring reaction mechanisms and parameters have been proposed [30–36]. Yet high-throughput biological data, generated by microarray experiments or protein expression profiling, are often not of sufficiently high resolution for using these techniques. To address these issues, a combination of mathematical modeling and experimental validations is required. Iterations of model construction, system analysis, and experimental validation improve accuracy of the model and lead to increased predictive power. In particular, the power to quantify gene expression with high temporal resolution at the population level or single cell level will likely complement high-throughput technologies in facilitating inference of reaction mechanisms and parameters [37–43].

In this chapter, we present methodologies on modeling, simulation, and analysis of natural and synthetic cellular networks. We note that different types of mathematical models are widely used. Here we limit our scope to kinetic models, which represent systems of interest as coupled chemical reactions. By so doing, we steer away from discussing other widely used mathematical models, such as Boolean models and those focusing on spatial dynamics. We illustrate construction of mathematical models of cellular networks with increasing complexity. Further, we highlight mathematical representations commonly used to describe such cellular networks and discuss common techniques for analyzing modeling results. Importantly, we show how to relate modeling results to real biological systems and to make predictions that can be validated by experiments. We use relatively simple, well-characterized systems to illustrate these processes.

6.2 Construction and Analysis of Kinetic Models

Construction of a kinetic model can be a daunting task for a system consisting of a large number of components with complex interactions. To build an experimentally tractable model, it is important to define the scope of abstraction. Once the scope is defined, a conventional approach begins with a minimal diagram that includes key components and interactions among them. Identification of the key components and interactions is based on the current knowledge of biology and frequently on intuition and experience. Depending on the focus of study, a modeler may choose to emphasize certain signaling pathways while deemphasizing less relevant ones. These processes often accompany “lumping” or deletion of molecular interactions or components. Once the diagram is completed, a minimal mathematical model is constructed from the information embedded in the diagram and is further refined or extended to reflect new hypotheses or experimental measurements. Simulation of the final model reveals the network dynamics, which in turn gives insights into the intrinsic design principles.

6.2.1 Parameter Estimation and Modeling Resources

A major challenge in model formulation is determination of reaction mechanisms and estimation of parameters. In some systems, the network behaviors are defined mostly by the architecture of the system. These systems are highly robust to a wide range of parameters. In others, system dynamics are determined not only by the architecture, but also the parameters, which are often poorly understood. Therefore, construction of a meaningful mathematical model of a biological pathway requires two critical elements: interactions between molecular species and the kinetics of the interactions.

As the first step, we need to know the interactions between the molecular species in the model. Several pathway databases are available for this purpose: EcoCyc [44], Kegg [45], ERGO [46], aMAZE [47], ExPASy [48], www.sbml.org, STKE (Sci), and Nature Signaling update (www.signaling-gateway.org). The pathways included in these databases are retrieved and constructed from specialized

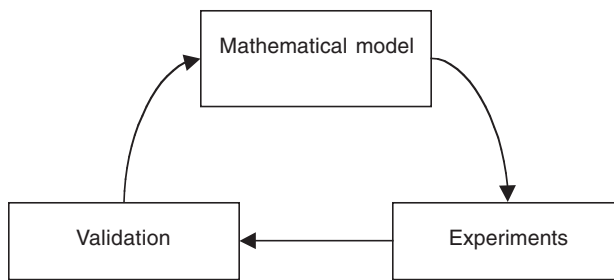


Figure 6.1 Refining models of biological networks. Iteration of model construction and experiments enable parameter and kinetics estimation and model refinement. The experimental data can be matched to the model with various computational methods.

databases such as GenBank, PDB, and EMBL. These pathway databases often provide detailed information on the molecular species. Next, we need to determine the kinetics of the interactions. In most cases, kinetic parameters are obtained from the literature data. Alternatively, we can use kinetic parameters from typical values, which can be based on values inferred from related process or even the experience of the modeler.







For every biological system, model construction usually goes through iterations of model construction, experimental validation, and model refinement (in terms of reaction mechanisms or parameter values) (Figure 6.1). These steps will be repeated until the mathematical model matches the experimental data to a satisfactory degree. This process can be considered as a special case of “reverse engineering” biological pathways. Additional methods, such as Bayesian [32], maximum likelihood [36], and genetic algorithms [33] can be used to infer more qualitative connectivity of biological networks from high-throughput experimental data.

6.2.2 A Modular Approach to Model Formulation

Modeling and analysis of complex biological systems may benefit from a modular approach, in which a biological system is conceptualized as a combination of smaller subnetworks with well-recognizable functions, termed motifs and modules [49, 50]. The distinction between motifs and modules is often based on the size difference but is not always clear-cut. We here use the two terms interchangeably. That is, we consider all small, conserved regulatory subnetworks as “modules,” classifiable on the basis of function, architecture, dynamics, and biochemical process. Such conceptualization may provide insight into the qualitative network dynamics at the systems level, and it helps clarify the modeling objective and generate qualitative hypotheses. In addition, it forms the basis for incorporating mathematical equations, with which more quantitative understanding can be attempted.

The dynamics of a module are governed by both network connectivity and associated parameter values. In general, increasing complexity in either variables or connectivity will result in more complex dynamics, and modules with feedback control may show properties that are difficult to grasp by intuition alone. Structures and properties of some well-defined feedback control modules are shown in Table 6.1, where we have summarized their key properties. For example, a module with one variable demonstrates either monostable or bistable properties with negative or

Table 6.1 Well-defined feedback modules involving negative, positive, or both types of regulation. In general, an increasing number of variables and more complex connectivity leads to richer dynamics.

Number of variables	Negative regulation only	Negative and positive regulation
1	 Monostable	 Bistable
2	 Bistable	 Oscillation
3	 Oscillation	 Oscillation ◦ ◦ Chaos

positive feedback control, respectively, but it is impossible to generate oscillations with a single variable in the absence of time delay. Monostable, bistable, or oscillatory behaviors, but not chaos, can be generated with a two-variable module. Modules with higher number of variables can demonstrate much richer dynamics such as chaos (Table 6.1) [49, 51, 52].

Various feedback control mechanisms confer properties useful for different biological functions. For example, negative feedback control is essential in homeostasis, a process of maintaining the system's internal environment in a steady state. Without feedback control, sudden external changes such as those in temperature or salinity may induce significant internal damages that can be fatal to a cell. Negative feedback control can buffer the impact of such changes and facilitate homeostasis [53]. In attempts to engineer gene circuits, this property has been used to reduce variations in gene expression [54]. In addition, negative feedback may increase the response speed of simple gene cascades [55].

Positive feedback can create bistable behaviors. The synthetic biology approach has been used to develop bistable switches whose overall molecular mechanism is based on autocatalysis of a single gene [56, 57]. These networks may be considered as synthetic models of their natural counterparts, such as signaling network controlling cell cycle regulation [58, 59] and regulation of the lac operon [60]. Bistable switches can also be realized in a positive feedback system by combining negative regulations. A recent study on a synthetic “toggle” switch, a two-component module in which two transcriptional repressors negatively regulate each other, is shown to achieve bistable switching behaviors [61]. A combination of negative or positive regulation between two or more components can give rise to oscillations. This was theoretically or experimentally characterized in *Escherichia coli* [62–65].

In addition to monostable, bistable, or oscillatory modules, network architectures with other connectivity have also been identified, and their properties and biological

significance have been characterized [49, 52, 66, 67]. Importantly, these modules often maintain similar functions across different species. For example, oscillator modules are the molecular mechanisms that underlie molecular, physiological, and behavioral rhythms [68, 69] or pattern formations [70], and bistability modules may govern the cell's entry into the cell cycle and be responsible for controlling cell differentiation [58, 71–74]. Thus, thorough analysis of a module in one context can provide insight into its functional roles under a wide spectrum of conditions.

6.2.3 Basic Kinetics

In kinetic modeling, a biological system is considered to be a series of chemical reactions, whose kinetics can be described by rate expressions. The system is often composed of multiple reactions, which occur through direct interactions among reactants. If these interactions are elementary reactions, their rates can be modeled following the mass action law. That is, the reaction rate is proportional to the product of reactant concentrations. However, most biological models are frequently formulated as consisting of more complex reaction mechanisms. One important class is enzyme-catalyzed reactions, which are critical for live systems where virtually all reactions are too slow to support life without enzymes. The enzymes provide a way to regulate reactions at appropriate rates and conditions.

A commonly used reaction model for enzymatic reactions is the Michaelis-Menten equation. In this reaction mechanism, one assumes that the enzyme is not consumed and the total concentration of enzyme stays constant. It only interacts directly with the substrate to form an enzyme-substrate complex, which leads to the synthesis of the product:



Assuming that the intermediate (ES) is at the quasi-steady-state and the substrate is in excess, we can derive the Michaelis-Menten equation:

$$\frac{dP}{dt} = \frac{V_{\max}[S]}{K_M + [S]} \quad 6.2$$

where V_{\max} is the maximal reaction rate ($k_2[E]_{\text{Total}}$, where $[E]_{\text{Total}}$ is the total enzyme concentration) and K_M is the Michaelis-Menten constant $\frac{(k_r + k_2)}{k_f}$.

Another recurring scheme in modeling cellular networks is the representation of gene expression. Expression of a single gene involves two basic steps: transcription and translation. This simplistic view of gene regulation starts with transcription, where the RNA polymerase binds the promoter of a gene to result in mRNA synthesis. The mRNA that carries coded information binds with ribosome, and the coded information is translated into protein [Figure 6.2(a)].

In real systems, gene expression can be regulated at multiple layers involving interactions among inducers, repressors, and operator sites. The interactions of these components lead to two general categories of transcriptional regulations: activation and repression. When an activator binds to the operator site, this complex leads to recruitment of RNA polymerase (RNAP) and synthesis of mRNA (Figure 6.2b). In

contrast, binding of a repressor will prevent initiation of transcription by blocking the RNAP. In the absence of cooperative interactions, such as dimerization and synergistic binding of transcription regulators to promoters, both types of regulation can be mathematically described by using Michaelis-Menten type of kinetics [Figure 6.2b, c].

If the transcription regulator acts as a dimer or multimer, and/or if it binds synergistically to multiple operator sites, transcription regulation can be modeled by higher-order expressions, such as the commonly used Hill kinetics:

$$\frac{dP}{dt} = \frac{V_{\max}[S]^n}{K_M^n + [S]^n} \quad 6.3$$

where n is called the Hill coefficient. For $n = 1$, Hill kinetics is the same as the Michaelis-Menten kinetics. However, for the response curve that has a different slope from what is predicted by Michaelis-Menten kinetics, n can be adjusted to fit the Hill kinetics curve. Detailed treatment of this can be found in [75, 76].

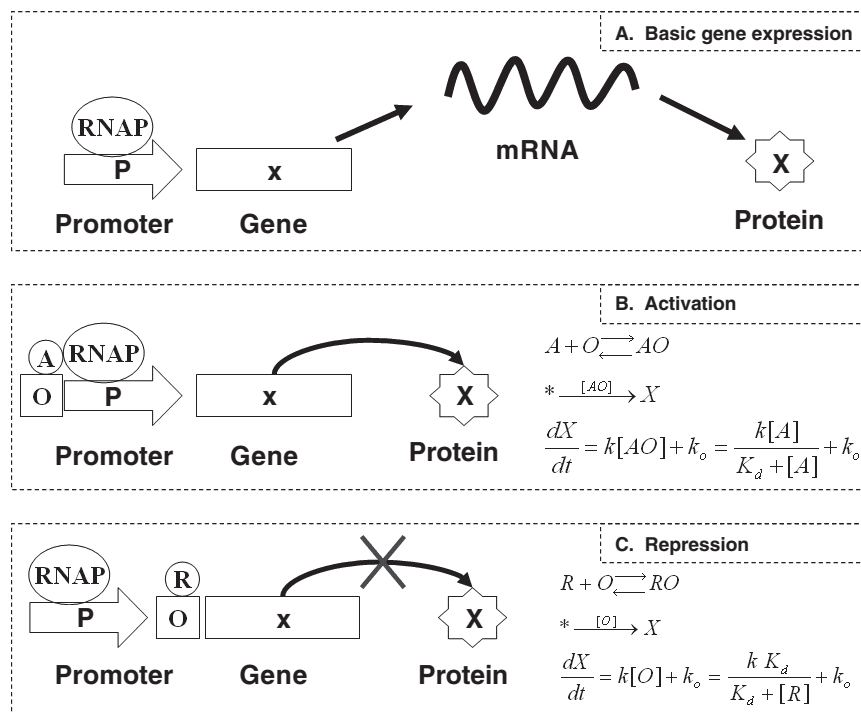


Figure 6.2 Modeling gene regulation. A simplified view of gene regulation is shown in (a). Initiation of mRNA synthesis can be triggered by either transcription activation (b) or transcription repression (c), which can be mathematically represented with the Michaelis-Menten type of kinetics. In transcription activation, the synthesis of mRNA depends on the amount of activators (A) bound to the operator (O). In contrast, the production of mRNA is repressed when the operator is bound to the repressor (R). In this case, the rate of transcription can be assumed to be proportional to the concentration of free operator sites. We assume that the RNA polymerase is not rate limiting and that translation and transcription steps are lumped together with an overall synthesis rate constant k . k_o is the basal protein synthesis rate constant, and K_d is the dissociation constant for the binding between A or R and O.

6.2.4 Deterministic Models

By treating each interaction as a chemical reaction, one can account for the production and depletion of each species by using an ordinary differential equation (ODE). A coupled system of ODEs that describes the dynamics of all elements in the network constitutes an integrated kinetic model. The general form of ODE systems can be written as:

$$\begin{aligned} \frac{dx_1}{dt} &= f_1(x_1, x_2, x_3, \dots, x_n) \\ &\vdots \\ \frac{dx_n}{dt} &= f_n(x_1, x_2, x_3, \dots, x_n) \end{aligned} \quad 6.4$$

where x_1, x_2, \dots, x_n represent levels of different interacting species, and f_1, f_2, \dots, f_n represent their corresponding rate expressions.

This representation often implies that the system dynamics occur in a well-stirred reactor in which bulk concentrations of the components are considered. Except for simple systems, an ODE-based kinetic model is often solved numerically using established methods [77–80]. Given the same parameter values, initial conditions, and simulation settings (e.g., error tolerance), different rounds of simulations will generate exactly the same temporal dynamics for each individual component. As such, an ODE model is also called a “deterministic” model. To assist in computational modeling research, a wide range of computational methods and tools have been developed for ODE systems [18, 81–86].

6.2.5 Cellular Noise and Stochastic Methods

ODE-based models are widely used to model dynamics of both natural and synthetic biological networks. For example, deterministic simulations predicted that a synthetic gene circuit of transcriptional repressors would cause sustained oscillations in gene expression [63]. Aspects of these predictions were verified in experiments where individual cells carrying the circuit displayed oscillatory behavior. However, the real system dynamics were quite stochastic when compared to deterministic simulation results from an ODE model. Specifically, oscillations in the repressilator occurred in only ~40% of individual cell lineages and were often out of phase with each other.

Such stochastic behavior is partially due to the intrinsically stochastic biochemical reactions among small numbers of molecules. These fluctuations in gene expression are often termed “noise” [87, 88]. In general, sources of noise include fluctuations in cellular components [40], transmitted noise from upstream genes [41], and other cellular processes unaccounted for by the model. Recently, the origin and propagation of noise in gene expression have been of central interest in many experimental studies [39, 43, 89–92].

The presence of cellular noise presents both a challenge and an opportunity for cellular function. On one hand, reliable function in the presence of noise requires strategies that reduce the impact of noise [89, 93]. For instance, one such mechanism that regulates noise is negative feedback, where the output from a system re-

duces its own output. In a biological context, this occurs when a protein inhibits its own expression by binding to its promoter. This mechanism has been shown to reduce noise in gene expression [54, 94]. On the other hand, noise may be beneficial by serving as a source for generating phenotypic diversity [93, 95], which can facilitate adaptation to changing environments or trigger cell differentiation [96].

Because of the important implications of noise for both natural and synthetic cellular networks, it is often useful to model stochastic dynamics. For a well-stirred, spatially homogeneous system, its stochastic temporal dynamics can be captured by a generic chemical master equation (CME) [97]:

$$\frac{\partial P(\tilde{x}, t | \tilde{x}_0, t_0)}{\partial t} = \sum_{j=1}^M a_j(\tilde{x} - \nu_j) \times P(\tilde{x} - \nu_j, t | \tilde{x}_0, t_0) - a_j(\tilde{x}) \times P(\tilde{x}, t | \tilde{x}_0, t_0) \quad 6.5$$

The first term of the equation describes probability of a species reacting at time t , while the second term describes the probability of a species remaining in its current state. \tilde{x} is a vector containing the number of molecules for each species. $P(\tilde{x}, t)$ gives the probability of the system in state \tilde{x} at time t . a_j is the propensity value of reaction j . ν_j is a vector containing the changes in state \tilde{x} caused by reaction j . \tilde{x}_0 and t_0 are the initial state and time respectively.

One can solve the CME analytically only for very simple systems. As the system size increases beyond a few reactions, the analytical solution of the CME becomes intractable. When the number of reactions and the number of molecules increase, the number of possible paths increases exponentially. Gillespie proposed a simple algorithm to solve the CME numerically using a Monte-Carlo method [98]. In this formulation, each reaction is assumed to be an elementary reaction, where collisions between reactant molecules directly lead to formation of products. The probability that a reaction happens is dependent on its reaction propensity (Table 6.2), which is analogous to a rate expression in ODE-based models.

The reaction propensity describes the probability of one molecule colliding with another molecule, which leads to the firing of a chemical reaction. Note that the reaction propensity for dimerization reactions is equal to $c x_A (x_A - 1)/2$ rather than $c x_A x_A$ because a molecule cannot react with itself. This presents a consistent interpretation of stochastic rate constants which are normally calculated from conventional rate constants [98]. Given the reaction propensity, we can now define the state of a species at time t . In order to follow the evolution of the states through time, we have to calculate which reaction (μ) is firing at time t and how much time (τ) the reaction requires. The probability of the firing event is shown in (6.6) and it can be calculated by using the schemes illustrated in Table 6.3.

$$P(\tau, \mu) = a_j \times \exp(-a_0 \times \tau) \quad 6.6$$

Table 6.2 Reaction propensity for stochastic methods. The reaction propensity describes probability of one molecule colliding with another.

Reaction	Propensity
$A \rightarrow B$	$c x_A$
$A + B \rightarrow C$	$c x_A x_B$
$2A \rightarrow B$	$c x_A (x_A - 1)/2$

Table 6.3 Pseudocode of Gillespie algorithm adapted from [98].

1. Calculate $a_0 = \sum_j^M a_j$
2. Generate two random numbers r_1 and r_2 from the uniform distribution (0, 1)
3. Compute $\tau = \frac{1}{a_0} \ln\left(\frac{1}{r_1}\right)$
4. Compute μ that satisfies $\sum_j^\mu a_j \geq r_2 \times a_0 \geq \sum_j^{\mu-1} a_j$
5. Execute reaction μ and advance time t by τ

Despite its simplicity, the computational cost of the Gillespie algorithm increases drastically with the number of reactions and the number of molecules in a system. The increment in computational cost is primarily due to the generation of random numbers (Step 2 in Table 6.3) and the enumeration of reactions to determine the next reaction (Step 4 in Table 6.3). For example, when the number of molecules is equal to 1×10^6 , τ will become excessively small (on the order of 1×10^{-6}), which then increases the number of time steps.

In order to simulate large-scale stochastic models, Gibson [99] proposed the “next reaction method” to improve computational efficiency of the Gillespie algorithm. The first improvement involves implementation of a tree data structure to store the reaction time of each reaction, which minimizes enumeration of the reactions at every time step. The second improvement uses a map data structure to minimize recalculation of the reaction propensity at every time step. The Gibson algorithm is significantly faster than the Gillespie algorithm for systems consisting of many reactions and many reacting species. It is also an exact algorithm in the sense that it satisfies the same basic assumptions as required by the Gillespie algorithm.

Several other algorithms were also proposed to improve computational speed of stochastic simulations. These algorithms are not exact and require users to predetermine an extra parameter that affects accuracy of the numerical solutions. Tau-leap algorithms [100] predict multiple firing of fast reactions and, hence, reduce the total number of time steps. Another class of algorithms is a hybrid algorithm [93, 101], which models fast reaction subsets using either ODEs or Langevin equations (see below), while treating slow reaction subsets with the stochastic algorithms.

An alternative, widely used stochastic method remains in the framework of differential equations by adding an appropriate noise term to each of the ODEs that describe the biological network. The resulting stochastic differential equations (SDEs) can then be solved numerically. Different formulations of SDEs can be established for different types of simulation applications. With appropriate assumptions, one can obtain a special type of SDEs, the chemical Langevin equation [102], which has been used to model a variety of cellular networks.

$$\frac{dX_i(t)}{dt} = \sum_{j=1}^M v_{ji} a_j[\mathbf{X}(t)] + \sum_{j=1}^M v_{ji} a_j^{1/2}[\mathbf{X}(t)] \Gamma_j(t) \quad 6.7$$

where $X_i(t)$ is the number of molecules of a molecular species in the system at time t and i refers to the specific molecular species ($i = 1, \dots, N$). $X(t) \equiv [X_1(t), \dots, X_N(t)]$ is the state of the entire system at time t , $a_j[X(t)]$ is the rate for a specific reaction or molecular interaction ($j = 1, \dots, M$); v_{ji} is a matrix describing the change in the number of molecules as a result of one molecular interaction. In other words, interactions that result in the synthesis of $X_i(t)$ are added and interactions that result in the degradation of $X_i(t)$ are subtracted; $\Gamma_j(t)$ are temporally uncorrelated, statistically independent Gaussian white noises.

SDEs are attractive in that they are computationally more efficient than the Gillespie algorithm and its derivatives. Also, by remaining in the framework of differential equations, they can facilitate in-depth analysis of system dynamics without always resorting to numerical simulations [103].

Regardless of the exact formulation of a stochastic algorithm, repeated rounds of stochastic simulations will generate different temporal dynamics for each individual species. One often uses an ensemble of simulated time courses to gain insights into noise characteristics, as well as how they are impacted by regulatory mechanisms. One way of quantifying noise in gene expression is to normalize the standard deviation of protein level with respect to the average protein level ($\gamma = \sigma/\mu$), where σ is the standard deviation of protein level and μ is the mean of protein level [40]. While this metric is direct and intuitive, some noise characteristics may be obscured by the more dominant small-number effects [89]. This may make it difficult to compare the noise of proteins that are being expressed at different levels. In this case, a more advantageous metric of quantifying noise is noise strength, or the variance of the protein level normalized with respect to the average protein level, $\zeta = \sigma^2/\mu$. Since gene expression is often controlled through transcription factors, noise levels can be compared among different genes regardless of their expression levels. This metric was recently used to analyze the relative contribution of transcription rates and translation rates to the noise characteristics of final protein products [103].

6.2.6 System Analysis Techniques

Given an integrated model, one can characterize the system behaviors using various analysis techniques, such as parametric sensitivity analysis and bifurcation analysis. These techniques allow for exploration of potential system dynamics and provide quantitative insights into emergent system behaviors, such as robustness. Such information is useful for revealing “design principles” of natural biological systems or guiding design and implementation of synthetic gene circuits.

6.2.6.1 Parametric Sensitivity Analysis

Sensitivity analysis is used to quantify changes in system behaviors in response to parameter changes. Different parameters may have varying impacts on the system dynamics and the degree of the impact can be quantified by a sensitivity value. A general method for computing the sensitivity value for an ODE system is

$$s(I; \phi_j) = \frac{\partial I}{\partial \phi_j} = \lim_{\Delta \phi_j \rightarrow 0} \frac{I(\phi_j + \Delta \phi_j) - I(\phi_j)}{\Delta \phi_j} \quad 6.8$$

where the sensitivity value is the ratio of change in the objective function of interest (I) to change in a parameter (ϕ_j).

Alternatively, the normalized form of sensitivity can be defined:

$$S(I; \phi_j) = \frac{\phi_j}{I} \times \frac{\partial I}{\partial \phi_j} = \frac{\partial \ln I}{\partial \ln \phi_j} = \frac{\phi_j}{I} \times s(I; \phi_j) \quad 6.9$$

This is also called logarithmic sensitivity. It is commonly used in metabolic control analysis [104] and has the feature of being dimensionless.

The objective function of interest is determined by the goals of the analysis. In the enzymatic synthesis of product that follows Michaelis-Menten kinetics, one may be interested in the change in the synthesis rate or in the steady-state product concentration as the Michaelis-Menten constant is varied. Therefore, there may be more than one sensitivity value for a given parameter. For an extensive treatment of sensitivity analysis, refer to [105].

Sensitivity analysis has been widely used in quantifying robustness of complex biological systems with respect to parametric perturbations [106–110]. In a complex system with a large number of parameters, the system behaviors may be robust to changes in various parameters. Especially, feedback controls and backup or compensation mechanisms in biological systems confer additional layers of robustness [14, 111–113]. Accurate identification of the underlying mechanisms for such robustness is challenging, since the system behaviors result from both parameters and system architecture. By distinguishing the impact of parameters from that of the architecture, sensitivity analysis provides a way to characterize system robustness. Such mathematical exploration of various system behaviors may serve as a guide in realizing system behaviors as desired experimentally. Specifically, if the parameters with high sensitivity values can be controlled, higher efficiency in biologically feasible experiment designs and data analysis can be achieved.

6.2.6.2 Bifurcation Analysis

While sensitivity analysis provides a quantitative measure of the dependence of system dynamics on parameters, bifurcation analysis focuses on a qualitative understanding of the system dynamics. Similar to sensitivity analysis, bifurcation analysis monitors changes in system behaviors in response to parameter changes, except that the goal is to explore *qualitative* changes in the systems dynamics. Bifurcation analysis is performed by varying a parameter until a qualitative change in dynamics is observed. The value at which this occurs is called the bifurcation point.

A quantitative measure of the stability can be achieved by a simple analytical method called linear stability analysis. This method provides a numerical value for the rate of decay to the stable steady-state solution from a small perturbation. Let us consider a model consisting of only one species,

$$\frac{dx}{dt} = f(x)$$

Linear stability analysis begins with steady-state solutions (x_s), which can be found by equating the right-hand side of the ODE expression to 0 and solving for the

species concentration of interest. Adding a small perturbation, $x = x_s + \delta(t)$, the right-hand side becomes

$$f(x) = f[x_s + \delta(t)] \xrightarrow{\text{Taylor's expansion}} f(x_s) + \delta(t)f'(x_s) + O[\delta(t)]^2$$

Assuming that the higher order terms $\{O[\delta(t)]^2\}$ are negligible and since $f(x_s)$ is 0, the system at steady state responds to small perturbations as $f(x) \approx \delta(t)f'(x_s)$. Since the left-hand side of the ODE equation

$$\frac{dx}{dt}$$

is equal to

$$\frac{d[x_s + \delta(t)]}{dt} = \frac{d\delta(t)}{dt}$$

the growth rate of perturbations is

$$\frac{d\delta(t)}{dt} = \delta(t)f'(x_s) \quad 6.10$$

Therefore, the perturbation will grow exponentially if $f'(x_s)$ is positive and will decay exponentially if $f'(x_s)$ is negative. Stability analysis of single-species systems is demonstrated in the gene expression example (See Section 3.1 for an example).

A bivariate system can be treated in a similar manner. For example, consider

$$\begin{aligned} \dot{x} &= f(x, y), & x &= x - \delta_x(t) \\ \dot{y} &= g(x, y), & y &= y - \delta_y(t) \end{aligned} \quad 6.11$$

where $\delta_x(t)$ and $\delta_y(t)$ denote a small disturbance from the steady-state solutions. Using the Taylor's expansion similar to the first-order system, we can approximate the growth rate of perturbations to be

$$\begin{pmatrix} \dot{\delta}_x \\ \dot{\delta}_y \end{pmatrix} = A \begin{pmatrix} \delta_x \\ \delta_y \end{pmatrix}, \text{ where } A = \begin{pmatrix} \frac{\partial f}{\partial x} & \frac{\partial f}{\partial y} \\ \frac{\partial g}{\partial x} & \frac{\partial g}{\partial y} \end{pmatrix}_{(x_s, y_s)} = \begin{pmatrix} a & b \\ c & d \end{pmatrix} \quad 6.12$$

where A is the Jacobian matrix at a steady state. The exponents of the growth rate are determined by eigenvalues λ of the matrix A , given by the characteristic equation $\det(A - \lambda I)$, where I is the identity matrix. Defining $\tau = \text{trace}(A) = a + d$ and $\Delta = \det(A) = ad - bc$, the eigenvalues are

$$\lambda_1 = \frac{\tau + \sqrt{\tau^2 - 4\Delta}}{2}, \quad \lambda_2 = \frac{\tau - \sqrt{\tau^2 - 4\Delta}}{2} \quad 6.13$$

Since the real part of an eigenvalue determines the rate at which the perturbation grows, the real part of both eigenvalues must be negative for the steady-state solutions to be stable. General analysis for yet more complex biological systems can be found in [114].

Varying the parameter of interest can create or destroy steady-state solutions, and the properties of these solutions can change. At bifurcation points where the network behaviors undergo a qualitative change, a stable steady-state solution may become unstable or vice versa. Also, a stable steady-state solution may diverge to two or no steady states. We demonstrate practical use of bifurcation analysis in modeling a synthetic population control circuit (see Section 6.3.2 for an example). For an extensive treatment of bifurcation analysis, refer to [115].

6.3 Case Studies

To illustrate the basic concepts and techniques outlined above, we here provide examples of kinetic modeling and analysis using three simple biological systems: expression of a single gene, a phosphorylation-dephosphorylation cycle composed of enzymatic reactions, and a synthetic population control circuit.

6.3.1 Expression of a Single Gene

Although gene expression is a complicated process that involves a number of components, we use the simplistic view as shown in Figure 6.3(a). Key assumptions in this view are that transcription of mRNA is constitutive with rate k and that translation of protein depends on the concentration of mRNA. Although the choice of parameters depends on many factors such as the gene of interest and the internal and external environment of gene expression, the commonly accepted estimation of parameters is sufficient for our gene expression model. Based on simplification and estimated parameters, mathematical models are constructed using ODE, SDE, and stochastic methods as shown in these models, implemented and simulated in a

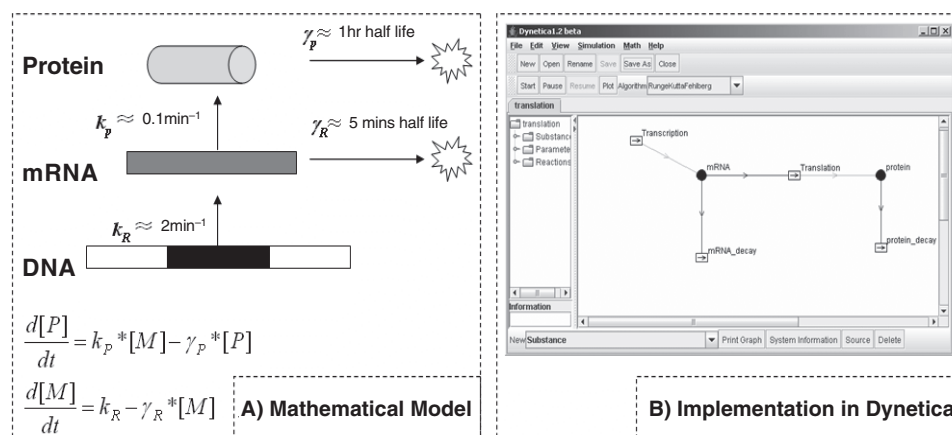


Figure 6.3 Modeling a single gene expression. A mathematical model is constructed based on our knowledge of the single gene expression and typical reaction parameters (a). While mRNA (M) is constitutively expressed with a rate constant of k_R , protein (P) is translated from mRNA with a rate constant of k_p . γ_p and γ_R are the degradation rate constants for the protein and the mRNA. This figure is adapted from [103]. (b) The model is implemented in a simulation and analysis software, *Dynetica* [82]. For direct comparison between stochastic and deterministic simulations, we chose to use molecular numbers as units for both proteins and mRNAs.

Table 6.4 Comparison between mathematical representation schemes for the gene expression.

ODE	SDE	Gillespie
<i>Reactions</i>	<i>Reactions</i>	<i>Reaction probability intensities^b</i>
$* \xrightarrow{k_R} \text{mRNA}$	$* \xrightarrow{k_R} \text{mRNA}$	$* \xrightarrow{c_R} \text{mRNA} \quad c_R$
$\text{mRNA} \xrightarrow{\gamma_R} *$	$\text{mRNA} \xrightarrow{\gamma_R} *$	$\text{mRNA} \xrightarrow{d_R} * \quad d_R N_R$
$* \xrightarrow{k_p[\text{mRNA}]} \text{protein}$	$* \xrightarrow{k_p[\text{mRNA}]} \text{protein}$	$* \xrightarrow{c_p N_R} \text{protein} \quad c_p N_R$
$\text{protein} \xrightarrow{\gamma_p} *$	$\text{protein} \xrightarrow{\gamma_p} *$	$\text{protein} \xrightarrow{d_p} * \quad d_p N_p$
<i>Ordinary differential equations</i>	<i>Stochastic differential equations^a</i>	<i>Gillespie Algorithm</i>
$\frac{d[\text{mRNA}]}{dt} = k_R - \gamma_R [\text{mRNA}]$	$\frac{d[\text{mRNA}]}{dt} = k_R - \gamma_R [\text{mRNA}] + \sqrt{k_R} \Gamma_1(t)$	• Calculate $a_0 = \sum_j^M a_j$
$\frac{d[\text{protein}]}{dt} = k_p * [\text{mRNA}] - \gamma_p [\text{protein}]$	$-\sqrt{\gamma_R [\text{mRNA}]} \Gamma_2(t)$	• Generate two random numbers r_1 and r_2
	$\frac{d[\text{protein}]}{dt} = k_p [\text{mRNA}] - \gamma_p [\text{protein}]$	• Compute $\tau = \frac{1}{a_0} \ln\left(\frac{1}{r_1}\right)$
	$+\sqrt{k_p [\text{mRNA}]} \Gamma_3(t) - \sqrt{\gamma_p [\text{protein}]} \Gamma_4(t)$	• Compute μ that satisfies $\sum_i^\mu a_i \geq r_2 \times a_0 \geq \sum_j^{\mu-1} a_j$
		• Execute reaction μ and advance time t by τ

^a $\Gamma_i(t)$ ($i = 1, \dots, 4$) are temporally uncorrelated Gaussian noise.

^b $c_R, d_R, c_p,$ and d_p are stochastic rate constants. $c_R = k_R N V$, where N is Avogadro's number and V is the cell volume. In this example, $d_R, c_p,$ and d_p are the same as their corresponding conventional rate constants. N_R and N_p are the numbers of mRNA and protein molecules.

graphic-based simulator Dynetica [82] [Figure 6.3(b)]. Also see (<http://labs.genome.duke.edu/YouLab/software/dynetica/index.php>).

As shown by simulation results in Figure 6.4, the stochastic simulations generated dynamics similar overall to that from a deterministic simulation, but their dynamics are noisy. The deterministic simulation also reveals that mRNA synthesis reaches steady state faster than protein production. Assuming a steady state for mRNA synthesis, we can carry out stability analysis of a steady state for gene expression. Equating the right-hand side of the ODE expression for mRNA in Table 6.4 to 0, we find the mRNA level at the steady state to be

$$\frac{K_R}{\gamma_R}$$

Then, the protein expression at the steady-state concentration of mRNA can be rewritten as

$$\frac{d[\text{protein}]}{dt} = \frac{k_p k_R}{\gamma_R} - \gamma_p [\text{protein}]$$

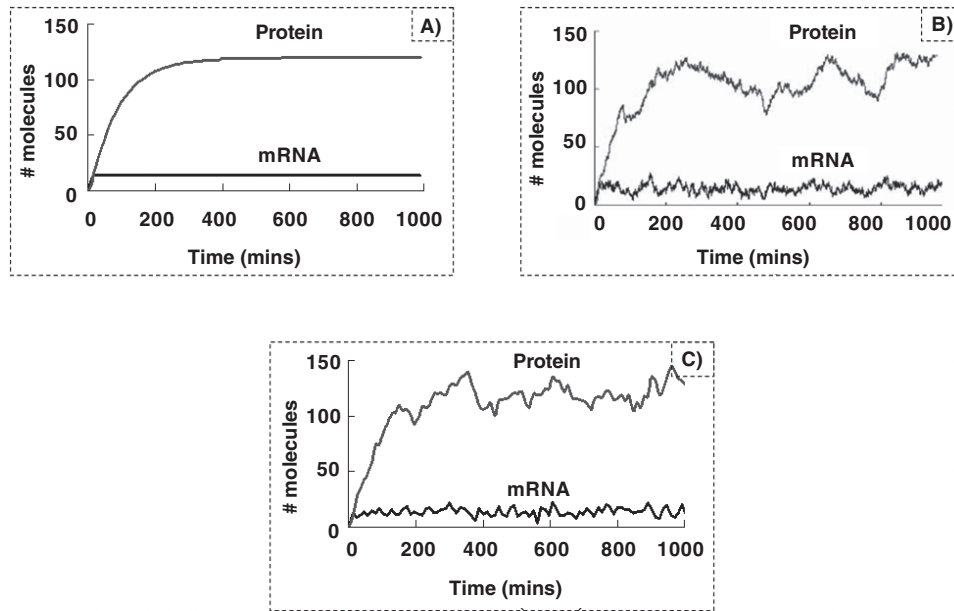


Figure 6.4 Simulation results of the model shown in Figure 6.3 by deterministic (a), SDE (b), and Gillespie (c) formulations.

When the decay rate ($\gamma_P[\text{protein}]$) matches the synthesis rate

$$\left(\frac{k_P k_R}{\gamma_R} \right)$$

the system is at a steady state. From (6.10), we can calculate the exponent for the growth rate of perturbation

$$\left(\frac{\partial f}{\partial P} \right)_{P=P_{SS}} = -\gamma_P < 0$$

where f is the right-hand side of the rate equation at the steady state, P is the protein level, and P_{SS} is the steady-state protein level. Since $f'(P_{SS})$ is negative, any perturbation around the steady state will decay at the rate of γ_P , indicating that the steady state is globally stable.

6.3.2 A Phosphorylation-dephosphorylation Cycle

Increasing in complexity, we analyze transient and steady-state behaviors of an enzyme-mediated phosphorylation cycle, which has been shown to demonstrate ultrasensitivity when the enzymes operate outside the region of first-order kinetics [116]. To construct a mathematical model, we begin with the conventional enzyme catalysis scheme where a protein switches between its phosphorylated and dephosphorylated forms (Figure 6.5). Assuming the enzymatic reactions follow the Michaelis-Menten kinetics and the total protein concentration is constant, we develop two ODE equations, which are implemented and simulated in Dynetica. Since

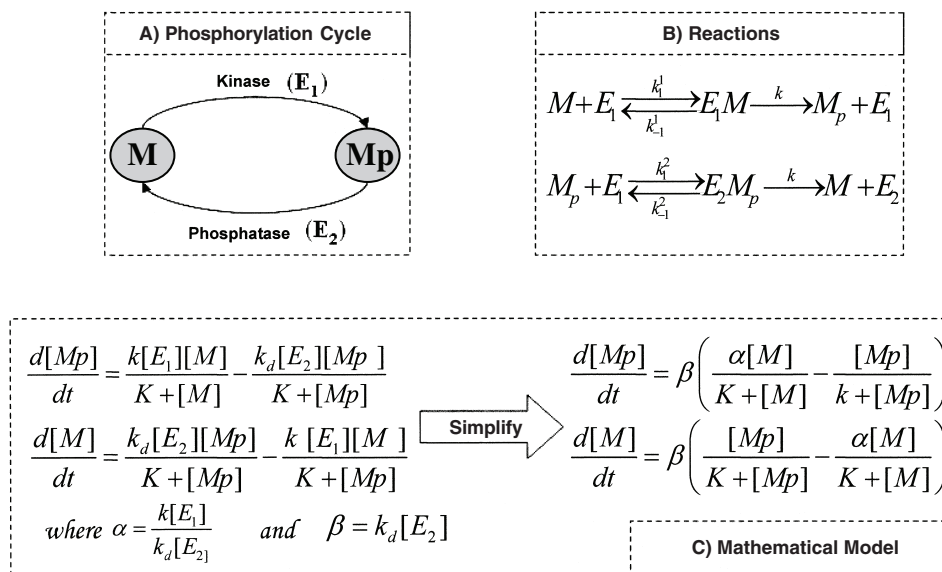


Figure 6.5 Modeling a phosphorylation-dephosphorylation cycle. An enzymatic modification cycle (a) of a protein between the dephosphorylated state M and the phosphorylated state M_p is mathematically modeled. k and k_d are rate constants for protein phosphorylation and dephosphorylation respectively. K is the Michaelis-Menten constant for the enzymatic modification cycle. Reaction schemes in (b) are converted to a set of ODEs (c) based on two assumptions: (1) Michaelis-Menten kinetics for the enzymatic reactions and (2) a constant total level of the protein.

the goal of modeling here is to identify general system behaviors of a phosphorylation cycle, we reason that a set of biologically feasible parameters in any phosphorylation cycles should be sufficient. Here, we choose parameters from the mitogen-activated protein kinase (MAPK) pathway [117], which has been extensively studied.

Assuming that the system starts with all protein in the unphosphorylated state, the protein will switch from the unphosphorylated state to the phosphorylated state over time, leading to a steady-state distribution of the protein in the two forms [Figure 6.6(a)]. This process is sensitive to α , a ratio between phosphorylation and dephosphorylation rates. When α is small, the amount of phosphorylated protein at the steady state is insignificant. However, more protein is converted as α becomes large. With very large α , the phosphorylation cycle becomes virtually irreversible, favoring the phosphorylated state.

The sensitivity analysis in Figure 6.6(b) shows the dependence of conversion on α . As the ratio of Michaelis-Menten constant to the total protein concentration, K , approaches 0, the dependence of conversion is ultrasensitive near α equal to 1. Then, the rate equation for the protein phosphorylation becomes

$$\frac{dMp}{dt} = \beta(\alpha - 1)$$

a zero-order rate expression that does not depend on concentrations of reactants, products, or enzymes. This dynamics is thus called zero-order ultrasensitivity. When the Michaelis-Menten constants are comparable to the total protein concentration (large K), the rate expression is first order and the ultrasensitivity at $\alpha = 1$

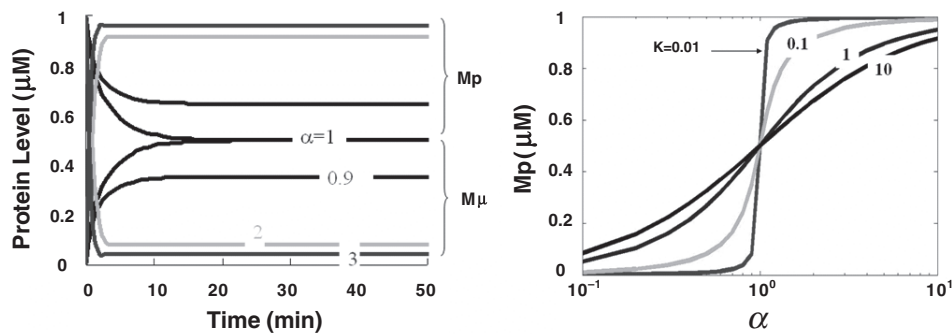


Figure 6.6 Simulation results for the model in Figure 6.5. Time-course results at varying α values show the dependence of conversion on the rate of phosphorylation and dephosphorylation (a). Protein conversion becomes ultrasensitive near $\alpha = 1$ for a sufficiently small Michaelis-Menten constant, while the sensitivity becomes weaker as K is increased (b).

becomes weaker. The time courses and sensitivity analysis in Figure 6.6 reveal two critical conditions to achieve ultrasensitivity: (1) α has to be near 1 and (2) the total protein concentration must be much greater than the Michaelis-Menten constants. That is, both kinase and phosphatase operate near saturation so that the overall reaction rate does not have a linear dependence on protein concentration.

We note that modeling can facilitate discovering design principles in biological systems. For example, ultrasensitivity is utilized in biological systems when sharp switching behavior is desired. A study of the mitogen-activated protein kinase (MAPK) pathway that combines both simulations and experiments has demonstrated ultrasensitivity. This work illustrates that the phosphorylation cycle mechanism under the two conditions is sufficient to generate a sharp switching behavior, whose Hill coefficient is estimated to be 5 [118]. At least two ways by which biological systems take advantage of ultrasensitivity can be speculated. In one scenario, a minor change in input will result in significant output when the system is operating near $\alpha = 1$. In the other scenario, a significant change in the input will have little impact on the output when α is much smaller or larger than 1. This may be useful in dealing with noisy signals, allowing the system to filter out noise [119].

6.3.3 A Synthetic Population Control Circuit

In addition to revealing dynamics of natural systems, modeling has become an indispensable tool for designing synthetic circuits [96, 120–125]. To illustrate this, we take as an example the synthetic population control circuit that we recently engineered [126, 127]. This circuit is based on a combination of two well-characterized modules: a quorum-sensing module and a killing module. Generally, we can develop an intuition about the circuit behavior, as the design is based on a combination of previously characterized modules. For example, the quorum-sensing module allows for cell-cell communication, where the cell density is broadcasted and detected by elements in the module. When the quorum-sensing module is coupled with a killing module, detection of high cell density by the quorum-sensing module activates killing of the cells. More specifically, the signal that diffuses across cell membranes to mediate communication is a small acyl-homoserine lactone (AHL)

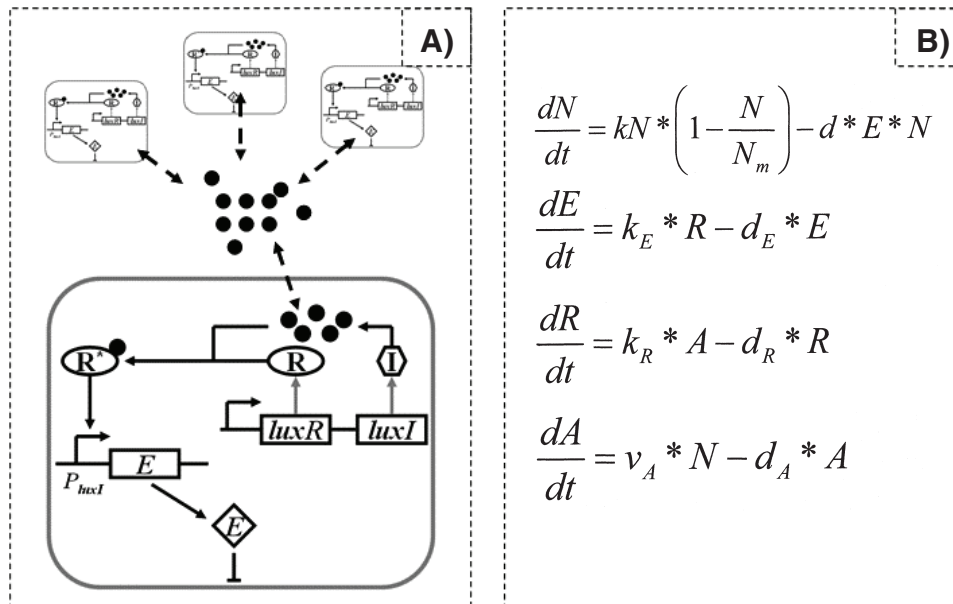


Figure 6.7 Modeling a synthetic population control circuit. (a) The cell density is broadcasted and detected by elements in the quorum-sensing module, and the killing of the cells is activated when high cell density is detected in the quorum-sensing module. The combination of the two modules allows for programmed population control. (b) An ODE-based kinetic model. Viable cell density N follows logistic growth with a specific growth rate k and a carrying capacity N_m . AHL (A), synthesized from the viable cells with a rate constant v_A , activates LuxR (R) with a rate constant k_R . Here d is the killing rate constant. k_E is the synthesis rate constant of E catalyzed by active LuxR and d_E , d_R , and d_A are the degradation rate constants for E , R , and A respectively. More details on the assumptions and the parameters can be found in [126, 127].

molecule synthesized by the LuxI protein. At high cell density, the AHL accumulates inside the cells and in the extracellular medium. At sufficiently high concentrations, it activates the LuxR transcriptional regulator, which in turn activates expression of the killer gene (E) under the control of a LuxI promoter ($pluxI$). Accumulation of the killer protein causes cell death. Based on this qualitative understanding of the programmed population control circuit, a set of ODE equations are formulated (Figure 6.7). The model is implemented, simulated, and analyzed in *XPP-AUT* [128].

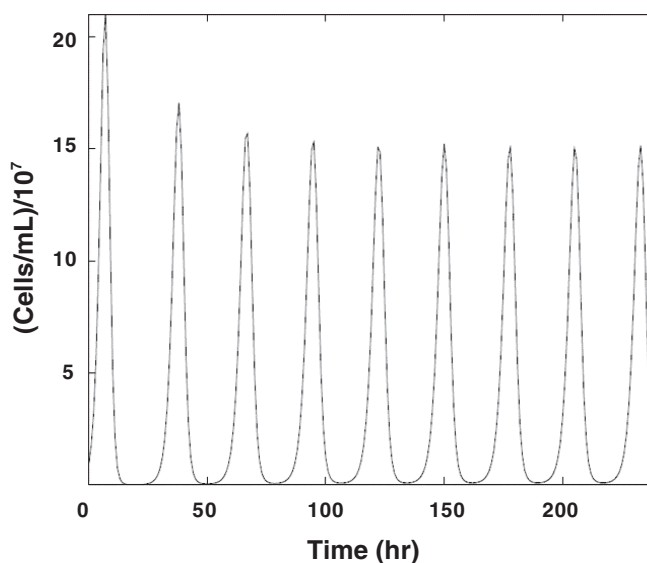
To improve predictive power of the mathematical model, the model parameters are adjusted to reflect experimental results, which are variable depending on experimental conditions. In the population control circuit, for example, the degradation of AHL is shown to be facilitated by the medium pH condition [129]. A series of experiments with varying medium pH were performed to obtain circuit parameters, as shown in Table 6.5 [127]. In this study, accurate representation of the experimental behaviors required adjustment of the AHL degradation rate calculated from experimental results.

Once the parameters are determined from experimental results, the understanding of the network structure can give insights into the system dynamics. For example, the population control system has a negative feedback control on the cell density by the killer protein. Such a structure has the potential to generate complex

Table 6.5 Effects of pH on circuit parameters (adapted from [127]).

Medium pH	k (b^{-1})	$N_m/10^9$ (CFU ml^{-1})	$N_s/10^7$ (CFU ml^{-1})	d_A (b^{-1})
6.2	0.885	1.25 ± 0.06	4.86 ± 0.02	0.274
6.6	0.928	1.17 ± 0.05	5.59 ± 0.03	0.304
7.0	0.970	1.24 ± 0.10	11.7 ± 0.6	0.639
7.4	0.897	1.16 ± 0.10	13.1 ± 0.6	0.791
7.8	0.936	1.20 ± 0.07	19.5 ± 1.3	1.19

dynamics, including oscillations. For certain biologically feasible parameters, our analysis shows that the model can indeed generate sustained oscillations over time. This prediction is consistent with experimental observations [126]. Further system stability analysis indicates that for $N \ll N_m$, there are two steady-state solutions. While the trivial steady state is always unstable, the nontrivial steady state is stable if degradation rates of LuxR, the killer protein, the AHL signal, and the microchemostat dilution rates are sufficiently large. However, decreases in these parameters destabilize the nontrivial steady state, leading to oscillations. This trend is captured in Figure 6.8. For each of these parameters, bifurcation analysis is carried out using *XPP-AUT* [Figure 6.9(a)]. In Figure 6.9b oscillations are observed for d_A less than 0.35, and the amplitude of the oscillations is the difference between the top and the bottom curves. High values of d_A (>0.35) stabilize the system, and the magnitude of oscillations decreases until damped oscillations occur [Figure 6.9(c)]. Further increases in d_A lead to stronger dampening of the oscillations that eventually eliminate oscillations [Figure 6.9(d)]. Similar stability analysis is carried out for the other parameters, and similar behaviors of the nontrivial steady-state solution are observed (Figure 6.10).

**Figure 6.8** Oscillation in the cell density over time for appropriate parameter values.

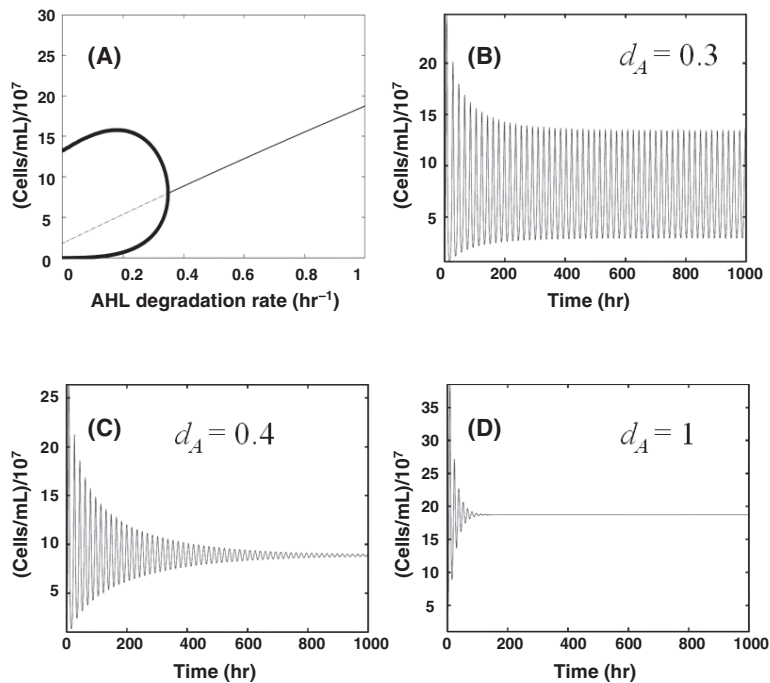


Figure 6.9 Bifurcation analysis. (a) Qualitative changes are observed in the dynamics as the AHL degradation rate constant (d_A) is varied. For sufficiently large d_A the steady-state solutions are stable as represented by the thin line. As d_A is decreased, the steady-state solutions become unstable (dashed line) and exhibit oscillations. The top and bottom branches of oscillations are indicated by the upper and lower curves respectively. For example, (b) oscillation in cell density is observed when d_A is sufficiently small (≤ 0.35). (c) The population undergoes damped oscillation in cell density for increased d_A . (d) Further increase in d_A stabilizes cell density.

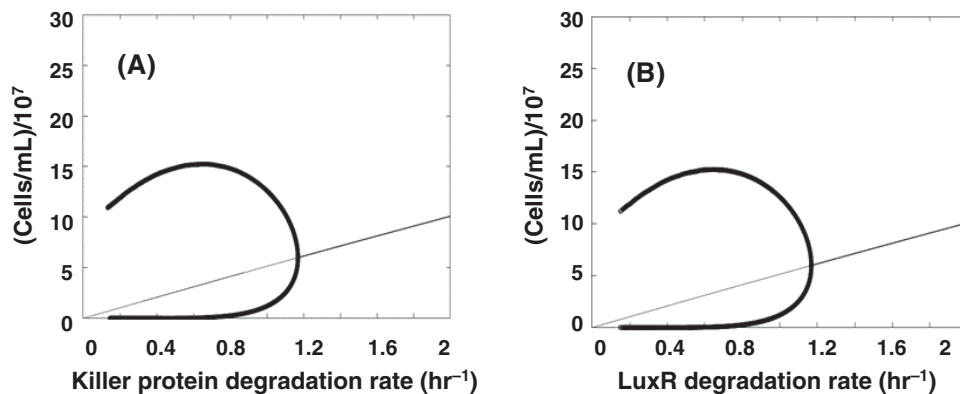


Figure 6.10 Further bifurcation analysis with rates for killer protein degradation (a) and LuxR degradation (b) is performed. Oscillations at sufficiently smaller rates diminish as the rates increase.

6.4 Conclusion

We have used relatively simple, well-characterized systems to illustrate construction and analysis of kinetic models. In these simple examples, we have demonstrated the significance of kinetic modeling not only for improved understanding of biological systems but also for improved predictions of cellular response to perturbations. We note that mathematical modeling is not limited to simple systems, but has also been used in more complex systems. Successful application of modeling has been demonstrated by numerous studies. The increase in the complexity of modeled systems suggests wider applicability of mathematical modeling. Integrated understanding of complex systems, whose dynamics cannot be conceptualized by intuition alone, can be achieved in a quantitative manner. Also, improved predictive power is particularly promising in the development of therapeutics, where system-level understanding is essential to minimize side effects and to precisely predict drug effects. Finally, modeling of cellular networks has become an integral part of the nascent field of synthetic biology. The combination of design, modeling, experimental implementation, and characterization of synthetic circuits or modules can provide substantial insights into the design principles of more complex natural biological systems and assist in the creation of artificial systems for practical applications.

References

- [1] Alemany, R., C. Balague, and D. T. Curiel, "Replicative adenoviruses for cancer therapy," *Nature Biotechnol.*, Vol. 18, No. 7, 2000, pp. 723–727.
- [2] Bischoff, J. R., et al., "An adenovirus mutant that replicates selectively in p53-deficient human tumor cells" [see comment], *Science*, 1996, Vol. 274, No. 5286, pp. 373–376.
- [3] Coffey M. C., et al., "Reovirus therapy of tumors with activated Ras pathway" [see comment], *Science*, Vol. 282, No. 5392, 1998, pp. 1332–1334.
- [4] Guillemard, V., and H. U. Saragovi, "Novel approaches for targeted cancer therapy," *Curr. Cancer Drug Targets*, Vol. 4, No. 4, 2004, pp. 313–326.
- [5] Jakubczak J. L., et al., "An oncolytic adenovirus selective for retinoblastoma tumor suppressor protein pathway-defective tumors: dependence on E1A, the E2F-1 promoter, and viral replication for selectivity and efficacy," *Cancer Res.*, Vol. 63, No. 7, 2003, pp. 1490–1499.
- [6] Nevins, J. R., "The Rb/E2F pathway and cancer," *Hum. Mol. Genet.*, Vol. 10, No. 7, 2001, pp. 699–703.
- [7] Rogulski, K. R., et al., "Double suicide gene therapy augments the antitumor activity of a replication-competent lytic adenovirus through enhanced cytotoxicity and radiosensitization," *Hum. Gene Therapy*, Vol. 11, No. 1, 2000, pp. 67–76.
- [8] Johnson, L., et al., "Selectively replicating adenoviruses targeting deregulated E2F activity are potent, systemic antitumor agents," *Cancer Cell*, Vol. 1, No. 4, 2002, pp. 325–337.
- [9] Khuri, F. R., et al., "A controlled trial of intratumoral ONYX-015, a selectively-replicating adenovirus, in combination with cisplatin and 5-fluorouracil in patients with recurrent head and neck cancer" [see comment], *Nat. Med.*, Vol. 6, No. 8, 2000, pp. 879–885.
- [10] Hastay, J., et al., "Computational studies of gene regulatory networks: in numero molecular biology," *Nat. Rev. Genet.*, Vol. 2, No. 4, 2001, pp. 268–279.
- [11] Ideker, T., L. Winslow, and A. Lauffenburger, "Bioengineering and Systems Biology," *Annals Biomed. Eng.*, Vol. 34, No. 2, 2006, p. 257.

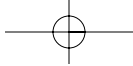
- [12] Neves, S. R., "Modeling of signaling networks," *BioEssays*, Vol. 24, No. 12, 2002, p. 1110.
- [13] Weston, A. D., "Systems biology, proteomics, and the future of health care: Toward predictive, preventative, and personalized medicine," *J. Proteome Res.*, Vol. 3, No. 2, 2004, p. 179.
- [14] Kitano, H., "Computational systems biology," *Nature*, Vol. 420, No. 6912, 2002, p. 206.
- [15] Rao, C. V., A. P. Arkin, "Control motifs for intracellular regulatory networks," *Annu. Rev. Biomed. Eng.*, Vol. 3, 2001, pp. 391–419.
- [16] Endy, D., and R. Brent, "Modelling cellular behaviour," *Nature*, Vol. 409, No. 6818, 2001, pp. 391–395.
- [17] Kholodenko, B. N., "Cell-signalling dynamics in time and space," *Nat. Rev. Mol. Cell Biol.*, Vol. 7, No. 3, 2006, pp. 165–176.
- [18] Alves, R., F. Antunes, and A. Salvador, "Tools for kinetic modeling of biochemical networks," *Nat. Biotech.*, Vol. 24, No. 6, 2006, p. 667.
- [19] You, L., "Toward computational systems biology," *Cell Biochem. Biophys.*, 40, No. 2, 2004, pp. 167–184.
- [20] Sasagawa, S., et al., "Prediction and validation of the distinct dynamics of transient and sustained ERK activation" [see comment]. *Nat. Cell Biol.*, Vol. 7, No. 4, 2005, pp. 365–373.
- [21] Schoeberl, B., et al., "Computational modeling of the dynamics of the MAP kinase cascade activated by surface and internalized EGF receptors," [see comment], *Nat. Biotechnol.*, Vol. 20, No. 4, 2002, pp. 370–375.
- [22] Bhalla, U. S., P. T. Ram, and R. Iyengar, "MAP kinase phosphatase as a locus of flexibility in a mitogen-activated protein kinase signaling network" [see comment], *Science*, Vol. 297, No. 5583, 2002, pp. 1018–1023.
- [23] Asthagiri, A. R., and D. A. Lauffenburger, "A computational study of feedback effects on signal dynamics in a mitogen-activated protein kinase (MAPK) pathway model," *Biotechnol. Progress*, Vol. 17, No. 2, 2001, pp. 227–239.
- [24] Bhalla, U. S., and R. Iyengar, "Emergent properties of networks of biological signaling pathways" [see comment], *Science*, Vol. 283, No. 5400, 1999, pp. 381–387.
- [25] Taniguchi, C. M., B. Emanuelli, and C. R. Kahn, "Critical nodes in signalling pathways: insights into insulin action," *Nat. Rev. Mol. Cell Biol.*, Vol. 7, No. 2, 2006, pp. 85–96.
- [26] Somogyi, R., and L. D. Greller, "The dynamics of molecular networks: applications to therapeutic discovery," *Drug Discovery Today*, Vol. 6, No. 24, 2001, pp. 1267.
- [27] Jackson, T. L., and H. M. Byrne, "A mathematical model to study the effects of drug resistance and vasculature on the response of solid tumors to chemotherapy," *Math. Biosci.*, Vol. 164, No. 1, 2000, pp. 17–38.
- [28] Butcher, E. C., E. L. Berg, and E. J. Kunkel, "Systems biology in drug discovery," *Nat. Biotechnol.*, Vol. 22, No. 10, 2004, pp. 1253–1259.
- [29] Oda, K., et al., "A comprehensive pathway map of epidermal growth factor receptor signaling," *Mol. Syst. Biol.*, Vol. 1, No. 1, 2005, msb4100014–E4100011.
- [30] Gardner, T. S., et al., "Inferring genetic networks and identifying compound mode of action via expression profiling," *Science*, Vol. 301, No. 5629, 2003, pp. 102–105.
- [31] Butte, A. J., and I. S. Kohane, "Mutual information relevance networks: functional genomic clustering using pairwise entropy measurements." *Pacific Symp. Biocomputing*, 2000, pp. 418–429.
- [32] Friedman, N., et al., "Using Bayesian networks to analyze expression data." *J. Comput. Biol.*, Vol. 7, No. 3-4, 2000, pp. 601–620.
- [33] Moles, C. G., P. Mendes, and J. R. Banga, "Parameter estimation in biochemical pathways: A comparison of global optimization methods," *Genome Res.*, Vol. 13, No. 11, 2003, pp. 2467–2474.

- [34] Arkin, A., P. Shen, and J. Ross, "A Test Case of Correlation Metric Construction of a Reaction Pathway from Measurements," *Science*, Vol. 277, No. 5330, 1997, pp. 1275–1279.
- [35] You, L., and J. Yin, "Patterns of regulation from mRNA and protein time series," *Metabolic Eng.*, Vol. 2, No. 3, 2000, pp. 210–217.
- [36] Ideker, T., et al., "Testing for differentially-expressed genes by maximum-likelihood analysis of microarray data," *J. Compu. Biol.*, Vol. 7, No. 6, 2000, pp. 805–817.
- [37] Ronen, M., et al., "Assigning numbers to the arrows: parameterizing a gene regulation network by using accurate expression kinetics," *Proc. Natl. Acad. Sci. USA*, Vol. 99, No. 16, 2002, pp. 10555–10560.
- [38] Guido, N. J., et al., "A bottom-up approach to gene regulation," *Nature*, Vol. 439, No. 7078, 2006, pp. 856–860.
- [39] Austin, D. W., et al., "Gene network shaping of inherent noise spectra," *Nature*, Vol. 439, No. 7076, 2006, pp. 608–611.
- [40] Elowitz, M. B., et al., "Stochastic gene expression in a single cell," *Science*, Vol. 297, No. 5584, 2002, pp. 1183–1186.
- [41] Pedraza, J. M., and A. van Oudenaarden, "Noise propagation in gene networks" [see comment], *Science*, Vol. 307, No. 5717, 2005, pp. 1965–1969.
- [42] Becskei, A., B. B. Kaufmann, and A. van Oudenaarden, "Contributions of low molecule number and chromosomal positioning to stochastic gene expression" [see comment], *Nat. Genet.*, Vol. 37, No. 9, 2005, pp. 937–944.
- [43] Rosenfeld, N., et al., "Gene regulation at the single-cell level," *Science*, Vol. 307, No. 5717, 2005, pp. 1962–1965.
- [44] Keseler, I. M., et al., "A comprehensive database resource for *Escherichia coli*," *Nucleic Acids Res.*, Vol. 33, Database issue, 2005, pp. D334–D337.
- [45] Kanehisa, M., et al., "From genomics to chemical genomics: new developments in KEGG," *Nucleic Acids Res.*, Vol. 34, Database issue, 2006, pp. D354–D357.
- [46] Overbeek, R., et al., "The ERGO genome analysis and discovery system," *Nucleic Acids Res.*, Vol. 31, No. 1, 2003, pp. 164–171.
- [47] Lemer, C., et al., "The aMAZE LightBench: a web interface to a relational database of cellular processes," *Nucleic Acids Res.*, Vol. 32, Database issue, 2004, pp. D443–D448.
- [48] Gasteiger, E., et al., "ExpASY: The proteomics server for in-depth protein knowledge and analysis," *Nucleic Acids Res.*, 31, No. 13, 2003, pp. 3784–3788.
- [49] Wolf, D. M., and A. P. Arkin, "Motifs, modules and games in bacteria," *Curr. Opinion Microbiol.*, Vol. 6, No. 2, 2003, pp. 125–134.
- [50] Hartwell, L. H., et al., "From molecular to modular cell biology," *Nature*, Vol. 402, Suppl. 6761, 1999, pp. C47–C52.
- [51] Romond, P.-C., et al., "Alternating Oscillations and Chaos in a Model of Two Coupled Biochemical Oscillators Driving Successive Phases of the Cell Cycle," *Annals NY Acad. Sci.*, Vol. 879, No. 1, 1999, pp. 180–193.
- [52] Tyson, J. J., K. C. Chen, and B. Novak, "Sniffers, buzzers, toggles and blinkers: dynamics of regulatory and signaling pathways in the cell," *Curr. Opinion Cell Biol.*, Vol. 15, No. 2, 2003, pp. 221–231.
- [53] Batchelor, E., T. J. Silhavy, and M. Goulian, "Continuous control in bacterial regulatory circuits," *J. Bacteriol.*, Vol. 186, No. 22, 2004, pp. 7618–7625.
- [54] Becskei, A., and L. Serrano, "Engineering stability in gene networks by autoregulation," *Nature*, Vol. 405, No. 6786, 2000, pp. 590–593.
- [55] Rosenfeld, N., M. B. Elowitz, and U. Alon, "Negative autoregulation speeds the response times of transcription networks," *J. Mol. Biol.*, Vol. 323, No. 5, 2002, pp. 785–793.
- [56] Becskei, A., B. Seraphin, and L. Serrano, "Positive feedback in eukaryotic gene networks: cell differentiation by graded to binary response conversion," *EMBO J.*, Vol. 20, No. 10, 2001, pp. 2528–2535.

- [57] Kramer, B. P., and M. Fussenegger, "Hysteresis in a synthetic mammalian gene network," *Proc. Natl. Acad. Sci. USA*, Vol. 102, No. 27, 2005, pp. 9517–9522.
- [58] Thron, C. D., "Bistable biochemical switching and the control of the events of the cell cycle," *Oncogene*, Vol. 15, No. 3, 1997, pp. 317–325.
- [59] Yao, G., et al., In preparation.
- [60] Acar, M., A. Becskei, and A. van Oudenaarden, "Enhancement of cellular memory by reducing stochastic transitions," *Nature*, Vol. 435, No. 7039, 2005, pp. 228–232.
- [61] Gardner, T. S., C. R. Cantor, and J. J. Collins, "Construction of a genetic toggle switch in *Escherichia coli*," *Nature*, Vol. 403, No. 6767, 2000, pp. 339–342.
- [62] Atkinson, M. R., et al., "Development of genetic circuitry exhibiting toggle switch or oscillatory behavior in *Escherichia coli*," *Cell*, Vol. 113, No. 5, 2003, pp. 597–607.
- [63] Elowitz, M. B., and S. Leibler, "A synthetic oscillatory network of transcriptional regulators," *Nature*, Vol. 403, No. 6767, 2000, pp. 335–338.
- [64] Fung, E., et al., "A synthetic gene-metabolic oscillator," *Nature*, 2005, Vol. 435, No. 7038, pp. 118–122.
- [65] Guantes, R., and J. F. Poyatos, "Dynamical Principles of Two-Component Genetic Oscillators," *PLoS Compu. Biol.*, Vol. 2, No. 3, 2006, p. e30.
- [66] Milo, R., et al., "Network motifs: simple building blocks of complex networks" [see comment], *Science*, Vol. 298, No. 5594, 2002, pp. 824–827.
- [67] Shen-Orr, S. S., et al., "Network motifs in the transcriptional regulation network of *Escherichia coli*," *Nat. Genet.*, Vol. 31, No. 1, 2002, pp. 64–68.
- [68] Stoleru, D., et al., "A resetting signal between *Drosophila* pacemakers synchronizes morning and evening activity," *Nature*, Vol. 438, No. 7065, 2005, pp. 238.
- [69] Levine, J. D., et al., "Signal analysis of behavioral and molecular cycles," *BMC Neurosci.*, Vol. 3, 2002, p. 1.
- [70] Meinhardt, H., "Pattern formation in biology: a comparison of models and experiments," *Reps. Progr. Physics*, Vol. 55, No. 6, 1992, p. 797.
- [71] Xiong, W., and J. E. Ferrell, Jr., "A positive-feedback-based bistable 'memory module' that governs a cell fate decision" [see comment], *Nature*, Vol. 426, No. 6965, 2003, pp. 460–465.
- [72] Tyson, J. J., and B. Novak, "Regulation of the eukaryotic cell cycle: molecular antagonism, hysteresis, and irreversible transitions," *J. Theoret. Biol.*, Vol. 210, No. 2, 2001, pp. 249–263.
- [73] Tyson, J. J., et al., "Checkpoints in the cell cycle from a modeler's perspective," *Progr. Cell Cycle Res.*, Vol. 1, 1995, pp. 1–8.
- [74] Pomerening, J. R., E. D. Sontag, and J. E. Ferrell, Jr., "Building a cell cycle oscillator: hysteresis and bistability in the activation of *Cdc2*," *Nat. Cell Biol.*, Vol. 5, No. 4, 2003, pp. 346–351.
- [75] Bintu, L., et al., "Transcriptional regulation by the numbers: applications," *Curr. Opinion Genet. Devel.*, 15, No. 2, 2005, pp. 125–135.
- [76] Bintu, L., et al., "Transcriptional regulation by the numbers: models," *Curr. Opinion Genet. Devel.*, 15, No. 2, 2005, pp. 116–124.
- [77] Mathews, J. H., and K. D. Fink, *Numerical Methods Using MATLAB*, 4th ed., Upper Saddle River, NJ: Pearson, 2004.
- [78] Atkinson, K. E., *An Introduction to Numerical Analysis*, 2nd ed., New York: Wiley, 1989.
- [79] Quarteroni, A., R. Sacco, and F. Saleri, *Numerical Mathematics*, New York: Springer, 2000.
- [80] Epperson, J. F., *An Introduction to Numerical Methods and Analysis*, New York: J. Wiley, 2002.
- [81] Slepchenko, B. M., et al., "Quantitative cell biology with the Virtual Cell," *Trends Cell Biol.*, Vol. 13, No. 11, 2003, pp. 570–576.

- [82] You, L., A. Hoonlor, and J. Yin, "Modeling biological systems using Dynetica—a simulator of dynamic networks," *Bioinformatics*, Vol. 19, No. 3, 2003, pp. 435–436.
- [83] Ramsey, S., D. Orrell, and H. Bolouri, "Dizzy: stochastic simulation of large-scale genetic regulatory networks," *J. Bioinformatics Compu. Biol.*, Vol. 3, No. 2, 2005, pp. 415–436.
- [84] Dhar, P., et al., "Cellware—a multi-algorithmic software for computational systems biology," *Bioinformatics*, Vol. 20, No. 8, 2004, pp. 1319–1321.
- [85] Hucka, M., et al., "The systems biology markup language (SBML): a medium for representation and exchange of biochemical network models," *Bioinformatics*, Vol. 19, No. 4, 2003, pp. 524–531.
- [86] Mendes, P., "Biochemistry by numbers: simulation of biochemical pathways with Gepasi 3," *Trends Biochem. Sci.*, Vol. 22, No. 9, 1997, pp. 361–363.
- [87] McAdams, H. H., and A. Arkin, "Stochastic mechanisms in gene expression," *Proc. Natl. Acad. Sci. USA*, Vol. 94, No. 3, 1997, pp. 814–819.
- [88] Arkin, A., J. Ross, and H. H. McAdams, "Stochastic kinetic analysis of developmental pathway bifurcation in phage lambda-infected *Escherichia coli* cells," *Genetics*, Vol. 149, No. 4, 1998, pp. 1633–1648.
- [89] Kaern, M., et al., "Stochasticity in gene expression: from theories to phenotypes," *Nat. Rev. Genet.*, Vol. 6, No. 6, 2005, pp. 451–464.
- [90] Hooshangi, S., S. Thiberge, and R. Weiss, "Ultrasensitivity and noise propagation in a synthetic transcriptional cascade," *Proc. Natl. Acad. Sci. USA*, Vol. 102, No. 10, 2005, pp. 3581–3586.
- [91] Raser, J. M., and E. K., "Control of stochasticity in eukaryotic gene expression," *Science*, Vol. 304, No. 5678, 2004, pp. 1811–1814.
- [92] Bar-Even, A., et al., "Noise in protein expression scales with natural protein abundance," *Nat. Genet.*, Vol. 38, No. 6, 2006, pp. 636–643.
- [93] Rao, C. V., D. M. Wolf, and A. P. Arkin, "Control, exploitation and tolerance of intracellular noise" [erratum appears in *Nature*, Vol. 421, No. 6919, 9 Jan. 2003, p. 190.], *Nature*, Vol. 420, No. 6912, 2002, pp. 231–237.
- [94] Savageau, M. A., "Comparison of classical and autogenous systems of regulation in inducible operons," *Nature*, Vol. 252, No. 5484, 1974, pp. 546–549.
- [95] Weinberger, L. S., et al., "Stochastic gene expression in a lentiviral positive-feedback loop: HIV-1 Tat fluctuations drive phenotypic diversity," *Cell*, Vol. 122, No. 2, 2005, pp. 169–182.
- [96] Suel, G. M., et al., "An excitable gene regulatory circuit induces transient cellular differentiation," *Nature*, Vol. 440, No. 7083, 2006, pp. 545–550.
- [97] Gillespie, D. T., "A rigorous derivation of the chemical master equation," *Physica A: Statistical and Theoretical Physics*, Vol. 188, No. 1-3, 1992, pp. 404.
- [98] Gillespie, D. T., "Exact stochastic simulation of coupled chemical reactions," *J. Phys. Chem.*, Vol. 81, No. 25, 1977, pp. 2340.
- [99] Gibson, M. A., and J. Bruck, "Efficient exact stochastic simulation of chemical systems with many species and many reactions," *J. Chem. Phys.*, Vol. 104, 2000, pp. 1876–1889.
- [100] Cao, Y., D. T. Gillespie, and L. R. Petzold, "Efficient step size selection for the tau-leaping simulation method," *J. Chem. Phys.*, Vol. 124, No. 4, 2006, p. 044109.
- [101] Haseltine, E. L., and J. B. Rawlings, "Approximate simulation of coupled fast and slow reactions stochastic chemical kinetics," *J. Chem. Phys.*, Vol. 117, No. 15, 2002, pp. 6959–6969.
- [102] Gillespie, D. T., "The chemical Langevin equation," *J. Chem. Phys.*, Vol. 113, No. 1, 2000, pp. 297–306.
- [103] Ozbudak, E. M., et al., "Regulation of noise in the expression of a single gene," *Nat. Genet.*, Vol. 31, No. 1, 2002, pp. 69–73.

- [104] Fell, D. A., "Metabolic control analysis: a survey of its theoretical and experimental development," *Biochem. J.*, Vol. 286, Pt. 2, 1992, pp. 313–330.
- [105] Varma, A., M. Morbidelli, and H. Wu, *Parametric Sensitivity in Chemical Systems*, Cambridge, UK/New York, NY: Cambridge Univ. Press, 1999.
- [106] Morohashi, M., et al., "Robustness as a measure of plausibility in models of biochemical networks," *J. Theoret. Biol.*, Vol. 216, No. 1, 2002, pp. 19–30.
- [107] Barkai, N., and S. Leibler, "Robustness in simple biochemical networks" [see comment], *Nature*, Vol. 387, No. 6636, 1997, pp. 913–917.
- [108] You, L., and J. Yin, "Dependence of epistasis on environment and mutation severity as revealed by in silico mutagenesis of phage $\tau 7$," *Genetics*, Vol. 160, No. 4, 2002, pp. 1273–1281.
- [109] You, L., and J. Yin, "Evolutionary design on a budget: robustness and optimality of bacteriophage T7," *IEEE Proc. Systems Biol.*, Vol. 153, No. 2, 2006, pp. 46–52.
- [110] Alon, U., et al., "Robustness in bacterial chemotaxis" [see comment], *Nature*, Vol. 397, No. 6715, 1999, pp. 168–171.
- [111] Freeman, M., "Feedback control of intercellular signalling in development," *Nature*, Vol. 408, No. 6810, 2000, p. 313.
- [112] Csete, M. E., and J. C. Doyle, "Reverse Engineering of Biological Complexity," *Science*, Vol. 295, No. 5560, 2002, pp. 1664–1669.
- [113] Carlson, J. M., and J. Doyle, "Complexity and robustness," *Proc. Natl. Acad. Sci. USA*, Vol. 99, No. 90001, 2002, pp. 2538–2545.
- [114] Murray, J. D., *Mathematical Biology*, 2nd. corr. ed., Berlin/New York: Springer-Verlag, 1993.
- [115] Strogatz, S. H., *Nonlinear Dynamics and Chaos: With Applications to Physics, Biology, Chemistry, and Engineering*, Reading, MA: Addison-Wesley Pub., 1994.
- [116] Goldbeter, A., and D. E. Koshland, Jr., "An amplified sensitivity arising from covalent modification in biological systems," *Proc. Natl. Acad. Sci. USA*, Vol. 78, No. 11, 1981, pp. 6840–6844.
- [117] Kholodenko, B. N., "Negative feedback and ultrasensitivity can bring about oscillations in the mitogen-activated protein kinase cascades," *Eur. J. Biochem.*, Vol. 267, No. 6, 2000, pp. 1583–1588.
- [118] Huang, C. Y., and J. E. Ferrell, Jr., "Ultrasensitivity in the mitogen-activated protein kinase cascade," *Proc. Natl. Acad. Sci. USA*, Vol. 93, No. 19, 1996, pp. 10078–10083.
- [119] Ferrell, J. E., Jr., "Tripping the switch fantastic: how a protein kinase cascade can convert graded inputs into switch-like outputs," *Trends Biochem. Sci.*, Vol. 21, No. 12, 1996, p. 460.
- [120] Tu, D., et al., "Engineering Gene Circuits: Foundations and applications," *Nanotechnol. Biotechnol. Med.*, 2006.
- [121] Church, G. M., "From systems biology to synthetic biology," *Mol. Syst. Biol.*, Vol. 1, No. 1, 2005, pp. msb4100007–E4100001.
- [122] Hastay, J., D. McMillen, and J. J. Collins, "Engineered gene circuits," *Nature*, Vol. 420, No. 6912, 2002, pp. 224–230.
- [123] Andrianantoandro, E., et al., "Synthetic biology: new engineering rules for an emerging discipline," *Mol. Syst. Biol.*, Vol. 2, 2006, p. E1.
- [124] Colman-Lerner, A., et al., "Regulated cell-to-cell variation in a cell-fate decision system," *Nature*, Vol. 437, No. 7059, 2005, pp. 699–706.
- [125] Endy, D., "Foundations for engineering biology," *Nature*, Vol. 438, No. 7067, 2005, p. 449.
- [126] Balagadde, F. K., et al., "Long-term monitoring of bacteria undergoing programmed population control in a microchemostat," *Science*, Vol. 309, No. 5731, 2005, pp. 137–140.



- [127] You, L., et al., "Programmed population control by cell-cell communication and regulated killing," *Nature*, Vol. 428, No. 6985, No., 2004, pp. 868–871.
- [128] Doedel, E. J., "AUTO: A program for the automatic bifurcation analysis of autonomous systems," *Dynamics*, Vol. 38, No. 9, 1983, p. 1493.
- [129] Schaefer, A. L., et al., "Detection, purification, and structural elucidation of the acylhomoserine lactone inducer of *Vibrio fischeri* luminescence and other related molecules," *Methods Enzymol.*, Vol. 305, 2000, pp. 288–301.

